www.sciencemag.org/content/349/6254/1306/suppl/DC1

Supplementary Materials for

Fractal atomic-level percolation in metallic glasses

David Z. Chen,* Crystal Y. Shi,† Qi An,† Qiaoshi Zeng, Wendy L. Mao, William A. Goddard III, Julia R. Greer

*Corresponding author. E-mail: dzchen@caltech.edu
†These authors contributed equally to this work.

Published 18 September 2015, *Science* **349**, 1306 (2015)
DOI: 10.1126/science.aab1233

This PDF file includes:

Other Supporting Online Material for this manuscript includes the following:
(available at www.sciencemag.org/content/349/6254/1306/suppl/DC1)

Databases S1 to S4 as zipped archives:
aab1233-Chen-SM-database-S1.rar
aab1233-Chen-SM-database-S2.rar
aab1233-Chen-SM-database-S3.rar
aab1233-Chen-SM-database-S4.rar

Materials and Methods

Sample preparation

~40μm-diameter cylindrical samples of as-cast $Cu_{46}Zr_{46}Al_5Be_3$ metallic glass were carved from a millimeter-diameter rod using the Focused Ion Beam (FIB) in an FEI Nova 200 DualBeam system. A slice was cut into the cross-section of the rod, and then a top-down circular mill was performed to obtain the cylindrical shape. The sample was extracted from its as-milled hole with the aid of an optical microscope.

XRD and TXM

Angle-dispersive X-ray diffraction were performed at beamline 16BM-D of the Advanced Photon Source (APS), Argonne National Laboratory (ANL) with a wavelength of 0.309846 Å. The sample was loaded into a 150 μm hole in a stainless steel gasket and compressed by diamonds anvils with 300 μm culets. Helium was used as the pressure-transmitting medium to guarantee hydrostatic pressure conditions. Loading was performed at the GeoSoilEnviroCARS of APS, ANL.

X-ray images of the sample were collected using a full field TXM installed at beam line 6-2 of the Stanford Synchrotron Radiation Lightsource (SSRL), SLAC National Accelerator Laboratory. The sample was cut into a cylinder with a smooth surface using the FIB and then loaded along with a ruby ball as pressure calibrant into a 120-micron diameter sample chamber in an X-ray transparent beryllium (Be) gasket with cubic BN/epoxy insert. Silicone oil was used as the pressure-transmitting medium. The sample was compressed between a pair of 400 micron culet diamond anvils in a cross diamond anvil cell (X-DAC) with a viewing angle of 152°. The incident x-ray cone beam was fixed at 9240 eV, which is above the Cu K absorption edge to maximize the absorption contrast. The 2D projection images were collected during rotation of the 152° viewing angle with 1° intervals for each pressure point.

3D reconstruction of 2D projection images was performed using the TXM-Wizard software (*40*). The algebraic reconstruction technique (ART) algorithm was applied to each sinogram with 20 iteration cycles. Segmentation and volume measurement was conducted using Avizo® (FEI Visualization Sciences Group). The relative volume change as a function of pressure can be precisely measured. By keeping the contrast threshold values consistent for all the pressures points, we determined that the error associated with the relative volume change to be within 1%.

Cluster analysis

Honeycutt-Anderson (HA) analysis was performed to isolate icosahedral clusters in our simulated system by focusing on arrangements with the 1551 index (*41*, *42*). This was done to illustrate the connectedness of the atomic arrangements within our model.

Atomic radii and packing fractions

We generated minimized crystal structures of pure face-centered cubic (FCC) Cu and pure hexagonal close-packed (HCP) Zr to obtain the atomic radii of each element, r_{Cu} = 1.278 Å and r_{Zr} = 1.5895 Å for FF_1. We also generated crystals of $Cu_{50}Zr_{50}$, B2—body-centered cubic with non-identical atoms, and found the Cu-Zr pair separation to be 2.83 Å, a value ~1.5% lower than $r_{Cu} + r_{Zr}$, suggesting that such measured atomic radii for this system are fairly robust to structural changes. Assuming the atomic radii for the glass to be similar, we obtained the room-temperature packing fractions of $Cu_{46}Zr_{54}$ using two different force fields: ϕ = 0.717 for FF_1 and 0.728 for FF_2.

The values for the $Ni_{80}Al_{20}$ system were obtained in a similar way.

Peak measurement

For the experimental and simulation diffraction peak analysis, r_i and q_i values were measured manually by either direct measurement near the peak or bisecting the full width at half maximum (FWHM) of the peak after performing a Bezier smoothing. Peaks were also measured automatically using the peak analysis tool in OriginPro® with a smoothing window of 30-50 points. These conditions gave the most consistent results. For second peaks that are convoluted, partial RDFs may be more accurate. When peak shoulders are encountered, such as in r_2, the measurement is taken on the peak with the shoulder ignored or over the FWHM after smoothing. This method is robust, as the exact location of the peak is not important for the evaluation of the power law exponent, only the relative peak positions are, provided no shape change occurs. Therefore, it is likely sufficient to maintain a self-consistent method of peak measurement.

Supplementary Text

Correlation length

$$\xi \propto |p - p_c|^{-\nu}, \quad \text{(Eq. 1)}$$

At $p = p_c$, ξ diverges, which signifies that the entire system is fractal with macroscopic pores. At $p < p_c$ and $p > p_c$, ξ is finite, and the system is only fractal on length scales shorter than the correlation length. At probabilities greater than the percolation threshold, $p > p_c$, the percolation cluster is defined by,

$$M(r) \propto \begin{cases} r^{D_f}, & r \ll \xi, \\ r^{D}, & r \gg \xi. \end{cases} \quad \text{(Eq. 2)}$$

In Eq. 2, we modified $M(r) \sim r^{D_f}$ to be represented by a piecewise equation that depends on ξ.

To test our hypothesis that there must be a length beyond which the samples no longer exhibit fractal behavior, we modified Eq. 2 to better represent the experimentally obtained volume, V, which is related to mass through density, and the interatomic spacing, r_i, where i is the peak number or neighbor number. This gives:

$$V(r) \propto r_i^{D_f}. \quad \text{(Eq. 3)}$$

Eq. 3 then becomes,

$$V(r) \propto \begin{cases} r_i^{D_f}, & i < \xi, \\ r_i^{D}, & i > \xi, \end{cases} \quad \text{(Eq. 4)}$$

with both i and ξ described by pair separation distances. Eq. 4 implies that analyzing the data at peak positions beyond the first neighbor in real space will eventually allow us to probe the long-range dimensionality, 3, rather than the short-range fractal dimension, ~2.5, consistent with our original hypothesis.

Crossover from hydrostatic pressure

The equivalence of the packing fraction, ϕ, and the occupancy probability, p, in continuum percolation models suggests that it may be possible to modify the correlation length, ξ, by changing ϕ. Eq. 1 (in main text) indicates that as ϕ increases for $\phi > \phi_c$, ξ decreases. Under such conditions, the pair separation distances shrink, and at sufficiently high pressures, the correlation length should shift to a value significantly less than 2, which may cause the observed crossover in measured power law exponent from ~2.5 to 3 for the third RDF peak to occur earlier, in the second RDF peak. However, r_2 and r_3 are often quite broad, with typical full-widths at half maximum (FWHM) of ~1 Å or greater. In practice, it is likely necessary to apply enough pressure to bring the correlation length to the trough in between r_1 and r_2, which we will call r_{1-2}, in order to observe a crossover in power law exponent for r_2. This may be because, in the case of $\xi > r_{1-2}$, many clusters in the system are large, with radii spanning at least two nearest neighbors, and the structural information from r_2 should contain these fractal clusters with power law exponent ~2.5. In the case of $\xi < r_{1-2}$, the average size of the clusters is more than ~15% smaller, and the number of clusters spanning two nearest neighbors or more reduces significantly such that the structural information contained in the second RDF peak is overwhelmingly homogeneous, with power law exponent ~3. For our data, a typical value for r_{1-2}/r_2 is ~0.85. This value, when multiplied by an initial correlation length of 2 gives ξ~1.7 as the expected value for the crossover length between r_1 and r_2. Based on this, we can estimate that peak values measured from a packing fraction or density increase in excess of 11-12% are necessary to observe the crossover in r_2 for both force fields.

The data for r_2 of the model $Cu_{46}Zr_{54}$ system is extended to high pressures for both FF_1 and FF_2 (Fig. S1). This reveals a distinct transition around 15 and 20 GPa, where the power law exponents obtained from the second nearest neighbor peak, r_2, in both force fields shift from ~2.5 to 3. This pressure condition relates to a packing fraction in the range of ~0.803-0.844, greater than a ~12-16% increase in density, with an ξ of ~1.6-1.7. This analysis is performed at high pressures, which may result in errors, as EAM force fields are not typically tested at high pressures.

Contribution from affine and non-affine atoms

While hydrostatic pressures result in strictly affine displacements of the atoms in crystalline materials, this is not true for amorphous materials, where local displacements can be non-affine even for elastic deformation in response to purely hydrostatic loads. In our simulated systems, these non-affine atoms, identified with the criterion Dmin < r1/2, where Dmin is from ref. (35 from main text), make up roughly 21.7% of the number fraction of total atoms at room temperature (300 K) and 10 GPa. To decouple the contributions of affine and non-affine atoms to the power law exponents of our systems, we removed the non-affine atoms before measuring peak positions in the RDFs. The results for these nominally affine systems are consistent with our results from the whole system (Fig. S2), suggesting that the emergence of fractal properties and crossover at higher peaks is not an effect of non-affine rearrangements during loading. Since the calculation of Dmin is highly sensitive to thermal fluctuations, the same analysis was performed at low temperatures (10 K) in order to enable a stricter displacement threshold to be imposed while retaining a large number of atoms for generating smooth RDFs. A threshold of Dmin < r1/5 was imposed, resulting in 31.3% 'non-affine' atoms at 10 K and 10 GPa (Fig. S3). Note that low temperature quantum effects are not captured by

molecular dynamics. The results were the same for an intermediate temperature of 50 K (not included). This shows that the crossover in power law exponent is robust to different temperatures and to affine/non-affine deformations.

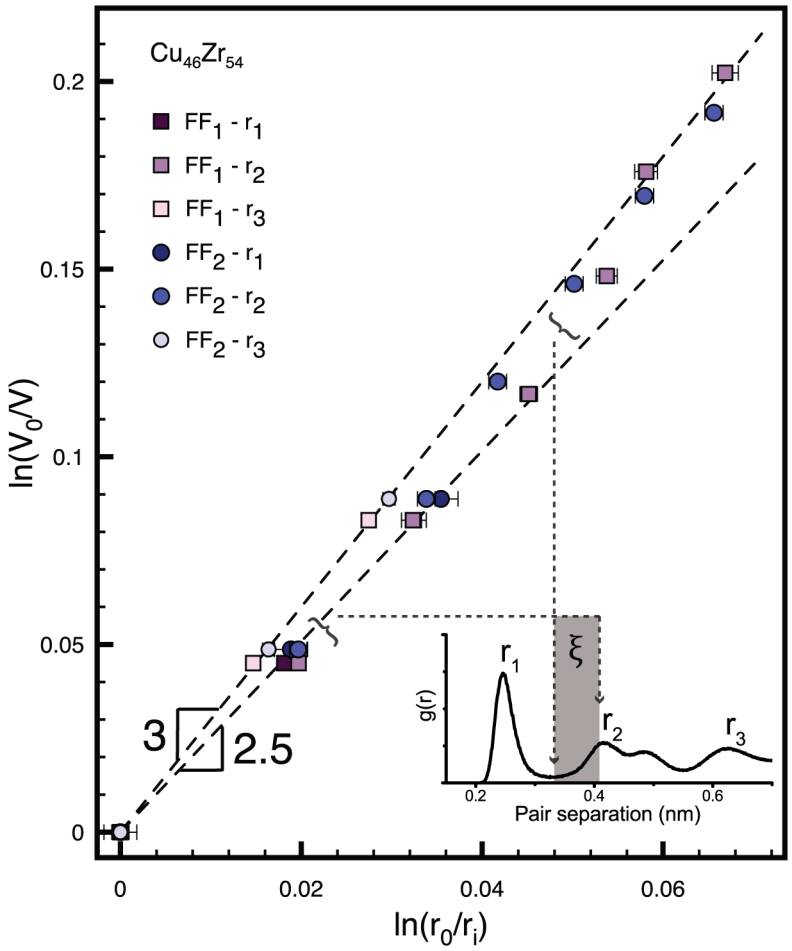

Fig. S1.

$Cu_{46}Zr_{54}$ FF_1 and FF_2 - both potentials show a crossover in dimensionality from ~2.5 to 3 between r_2 and r_3. This transition can also be induced in r_2 by increasing packing density using higher hydrostatic pressures (> 15 GPa). Each point is taken at 5 GPa intervals. Inset diagram shows an illustrative (NiAl) RDF curve with the shift in correlation length ξ highlighted by dotted grey arrows and grey box. As V_0/V increases, ξ decreases. Crossover occurs when ξ reaches the trough between r_1 and r_2.

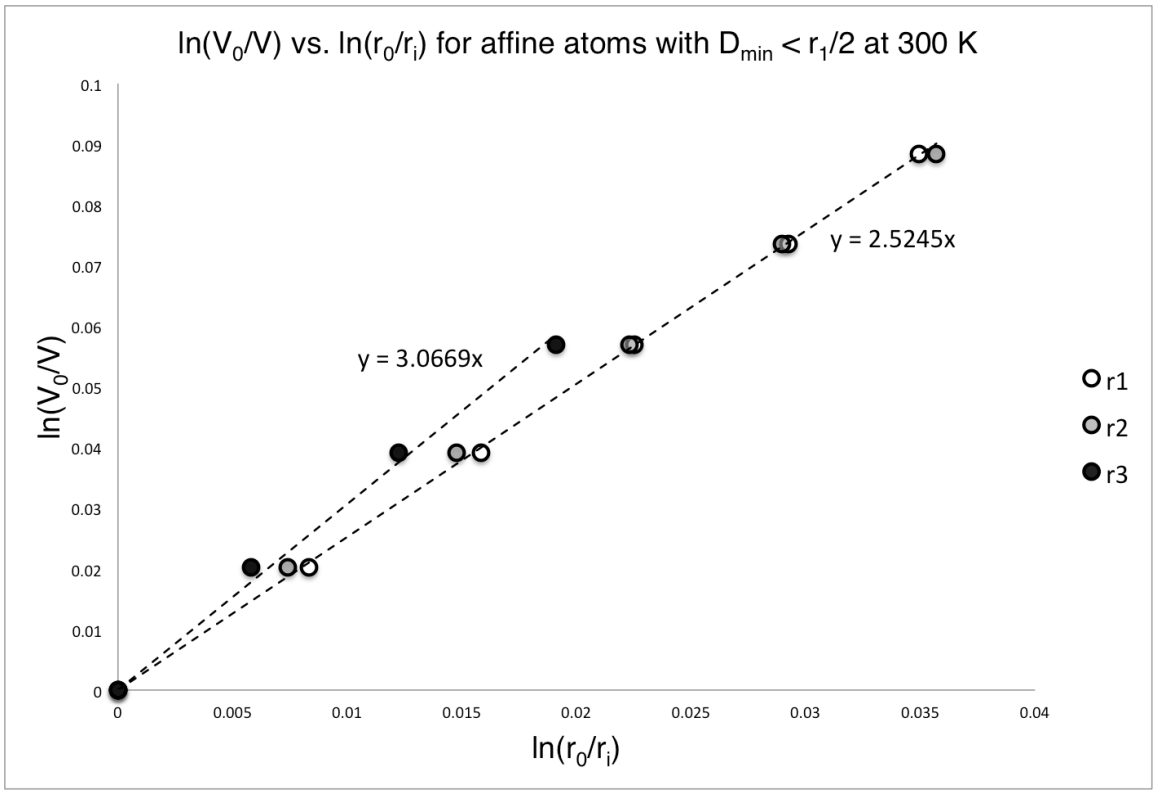

Fig. S2.

Power law exponent for isolated affine atoms in MD simulations defined by $D_{min} < r_1/2$ (35) at 300 K and 0-10 GPa. Results are consistent with those from the whole system, indicating that the measured fractal exponents are not from non-affine rearrangements under hydrostatic pressure.

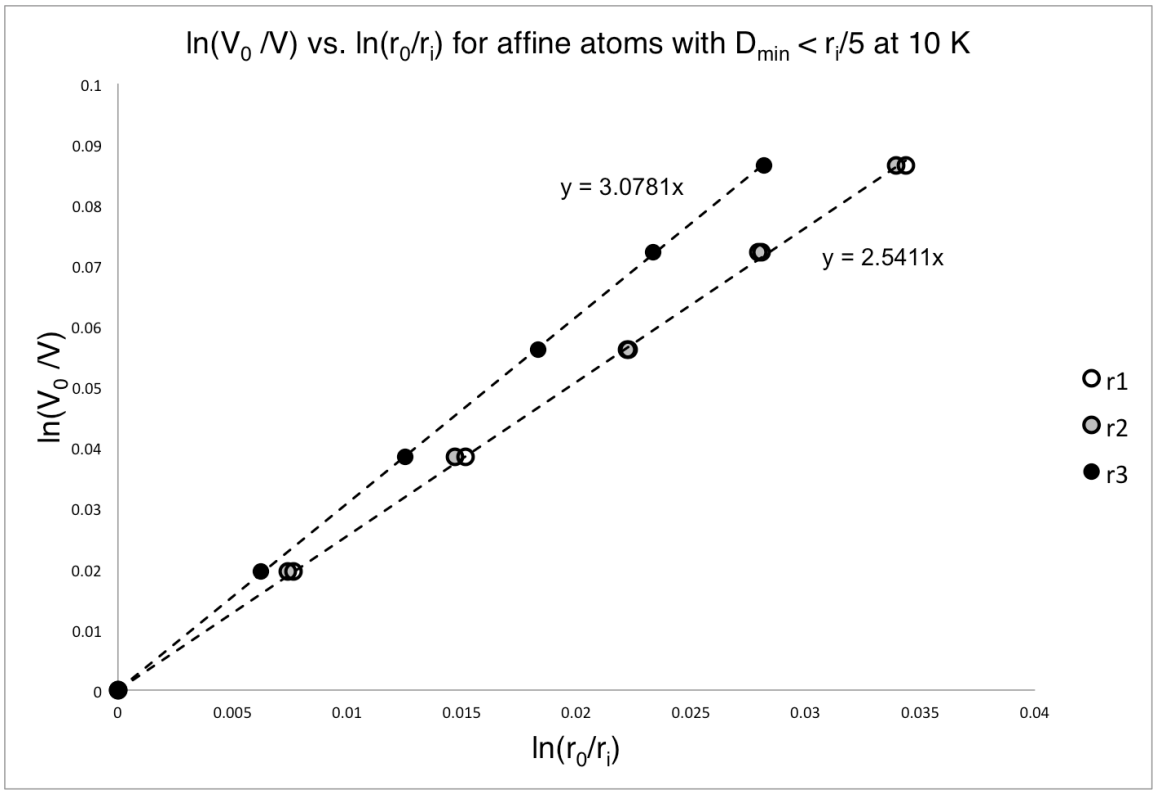

Fig. S3.

Power law exponent for isolated affine atoms in MD simulations defined by $D_{min} < r_1/5$ (35) at 10 K and 0-10 GPa. Results are consistent with those from the whole system, indicating that the measured fractal exponents are not from non-affine rearrangements under hydrostatic pressure.

Additional Data table S1 (separate file)

Diffraction data for the $Cu_{46}Zr_{46}Al_5Be_3$ sample

Additional Data table S2 (separate file)

RDF data for the $Cu_{46}Zr_{54}$ MD sample using FF_1

Additional Data table S3 (separate file)

RDF data for the $Cu_{46}Zr_{54}$ MD sample using FF_2

Additional Data table S4 (separate file)

RDF data for the $Ni_{80}Al_{20}$ MD sample